Acta Cryst. (1959). **12**, 1015

On the Crystal Chemistry of Normal Valence Compounds

BY E. MOOSER AND W. B. PEARSON

The Division of Pure Physics, National Research Council, Ottawa, Canada

(*Received* 12 *February* 1959 *and in revised form* 28 *April* 1959)

A new classification of the crystal structures of normal valence compounds with simple atomic ratios is discussed. This classification is based on two atomic parameters which gauge the directional properties of the bonds in a compound. The parameters are (1) the average principal quantum number, $\overline{n}$, of the valence shell of the component atoms and (2) the difference, Δx, between the electronegativities of anion and cation. It is shown that the most common structures of compounds of composition A_iX_j ($i, j = 1, 2, 3$) occur only in certain well defined regions of a $\overline{n}$ versus Δx diagram, and the proposed classification, therefore, is of considerable help in understanding and predicting the structures of normal valence compounds.

1. Introduction

The relationships between the chemical composition and the crystal structures of solids which so far have been discussed in the literature (see e.g. Evans, 1939; Hume-Rothery & Raynor, 1954; Laves, 1956) are mostly concerned with metals and alloys or with ionic compounds, little attention having been given to covalent structures. However, numerous investigations of semiconducting materials carried out over the last decade have stimulated physicists to take new interest in covalent phases formed at simple atomic ratios. The bonding in metallic and ionic phases is essentially nondirectional and the parameters used in classifying their structures are inappropriate for discussing covalent structures in which bonds with strongly pronounced directional properties are formed. The new classification of 'normal valence compounds' (i.e. covalent as well as ionic phases) which we are to discuss in the present paper is based on two parameters which gauge the directional properties of the bonds and in particular allow a description of the transition from covalent towards ionic and towards metallic bonding. These parameters are the average principal quantum number of the valence electrons of the component atoms of a compound and the difference between the electronegativities of anion and cation.

According to Dehlinger (1955) the principal quantum number n of the valence shell of an atom is a measure of the directional character of the bonds formed by this atom with atoms of the same kind (see also Mooser & Pearson, 1957). As n increases, the atomic orbitals involved in the bond formation and hence the bonds themselves gradually lose their directional properties. By introducing a suitable average quantum number $\overline{n}$ this relationship can be extended to the bonds formed between unlike atoms i.e. to the bonds in compounds. For our purposes we define:

$$\overline{n} = \Sigma c_i n_i / \Sigma c_i$$

where n_i is the principal quantum number of the valence electrons of the atom of kind i and c_i is the number, per formula unit, of atoms of this kind.

In compounds the directional character of the bonds does not, however, depend only on $\overline{n}$ but also on the electronegativity difference Δx because, whatever the value of $\overline{n}$, the bonds become increasingly ionic and hence more and more nondirectional as Δx increases.

In order to include in our discussion compounds with more than two components we define

$$\Delta x = |\overline{x}_{\text{anion}} - \overline{x}_{\text{cation}}|$$

where $\overline{x}_{\text{anion}}$ and $\overline{x}_{\text{cation}}$ are the arithmetic means of the anion and cation electronegativities. All Δx values have been calculated from the electronegativities given by Gordy & Thomas (1956).

The influence of $\overline{n}$ and Δx on the bonds in solids is reflected by the physical properties of the solids. Thus, for example, a change from insulating to semiconducting and finally to metallic properties is observed in the 4th Group of the Periodic Table, on going from diamond ($\overline{n}=2$) to lead ($\overline{n}=6$). This dependence of the electrical properties of the IV *B* elements on $\overline{n}$ illustrates a rule which holds for all elements to the right of the Zintl border and for all valence compounds, so that $\overline{n}$ can be considered as a measure of the 'degree of metallization' of these solids. The dependence of the electrical properties on Δx on the other hand is illustrated by the series Si, AlP, MgS and NaCl ($\overline{n}=3$) in which the conduction mechanism gradually changes from semiconductivity to ionic conductivity as the value of Δx increases from 0 to 2·1. It should be noted that because of these relationships the parameters $\overline{n}$ and Δx are of interest also in establishing empirical rules relating the activation energies and charge carrier mobilities of semiconductors to their chemical composition (see e.g. Pearson, 1959).

2. Discussion of various structures

The structures containing *covalent* (i.e. *directed*) bonds are as a rule readily recognizable from their characteristic coordination configurations. Before discussing specific structures we should, however, briefly summarize the characteristic features of *nondirectionally* bonded structures. According to Laves (1956) these features are (*a*) the best possible filling of space, (*b*) the highest possible symmetry and (*c*) the highest dimension of the connections (i.e. the networks formed by the links between nearest neighbours in a structure). Thus, as we go from directionally bonded towards metallic or ionic structures we will in general find more closely packed structures in which the component atoms have a higher coordination. Moreover, chain and layer structures whose connections are one- and two-dimensional respectively, will normally be met only in phases in which the bonding has a considerable covalent character.

(*a*) *Compounds of composition AX*

The most common structure types adopted by normal valence compounds of composition AX are the rocksalt type ($B1$), the zincblende type ($B3$) and the wurtzite type ($B4$). (For a brief description of the various structure types discussed in this paper see the Appendix.) With a few exceptions which will be discussed shortly, all phases known to crystallize in these structures have been plotted in Fig. 1 in terms of their average principal quantum numbers, $\bar{n}$, and their electronegativity differences, Δx. Also plotted in Fig. 1 are the chalcopyrite phases ($E1_1$ type) of composition ABX_2 whose structure can be regarded as a superlattice of the zincblende structure. Fig. 1 clearly demonstrates the remarkably sharp separation which occurs in an $\bar{n}$ versus Δx plot between the tetrahedrally coordinated structures and the octahedrally coordinated rocksalt structure. The form of the borderline between these phases indicates that the Δx values for which the higher coordinated rocksalt structure becomes energetically favorable depend on the 'degree of metallization' of the compound as measured by the average quantum number $\bar{n}$. From this and from the discussion given above, it follows that a compound crystallizes in the rocksalt structure not because the bonds are ionic but rather because they are nondirectional. Nevertheless there are some twelve compounds which crystallize in the rocksalt structure or in distorted forms thereof ($B16$, $B29$) even though their position

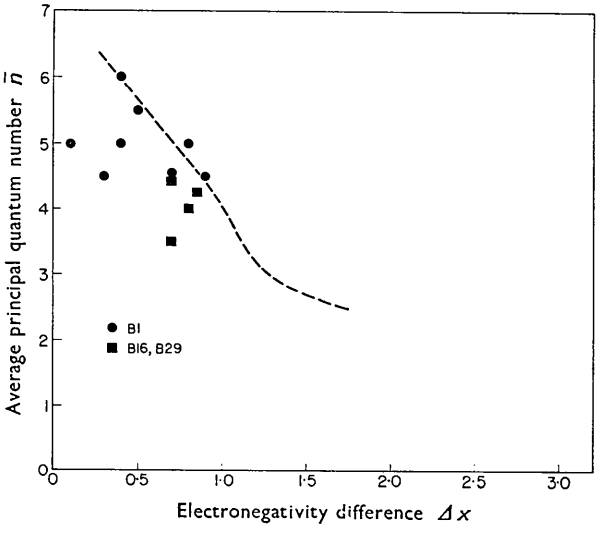

Fig. 2. $A^{IV}X^{V}$ and $A^{IV}X^{VI}$ compounds crystallizing in the rocksalt structure and in related structure types.

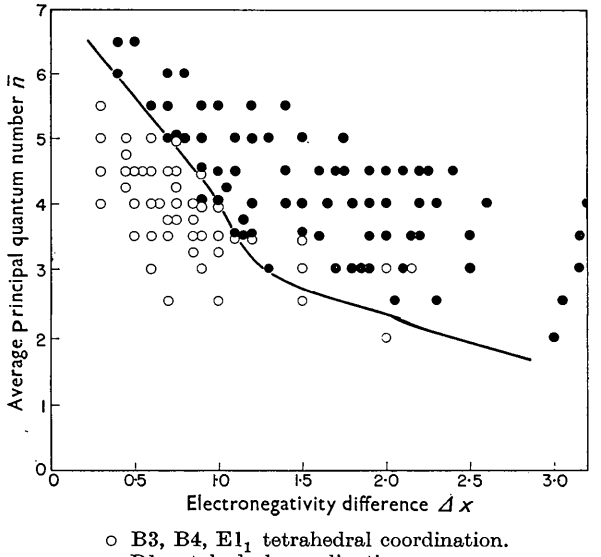

○ B3, B4, $E1_1$ tetrahedral coordination.
● B1 octahedral coordination.

Fig. 1. AX structures with tetrahedral and octahedral coordination.

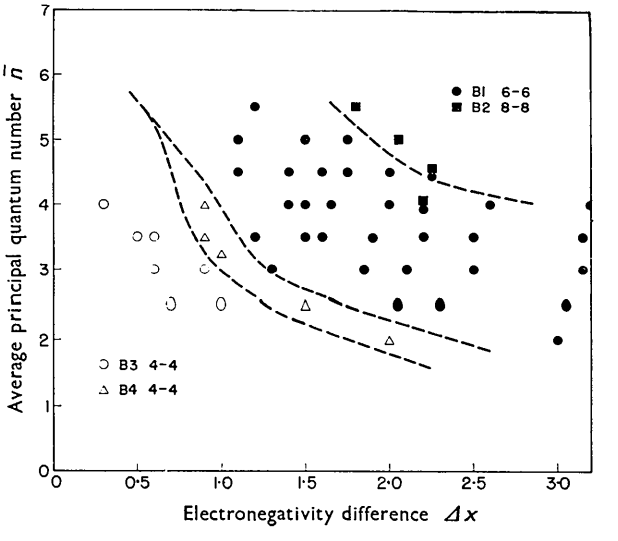

Fig. 3. AX compounds containing A group cations. The numbers behind the different structure types indicate the coordination configuration.

in a $\bar{n}$ versus Δx plot indicates directional rather than nondirectional bonds (Fig. 2). This anomaly is, however, understood since in these $A^{IV}X^{V}$ and $A^{IV}X^{VI}$ compounds the (heavy) Group IV cations are in their lower valence state retaining an unshared pair of s electrons and are thus unable to hybridize sp^3 tetrahedral bonds. Instead p resonance bonds form, the octahedral coordination configuration of which fits well into the symmetry of the rocksalt structure (see e.g. Krebs & Schottky, 1954).

There is a second group of compounds which fails to follow the systematics outlined in Fig. 1. Many of the *interstitial* hydrides, borides, carbides and nitrides of the transition elements which adopt the rocksalt structure lie well within the 'tetrahedral region' of the $\bar{n}$ versus Δx plot. This is due to the fact that interstitial phases are not normal valence compounds: they form because a close-packed array of large metal atoms can readily accommodate small atoms in its octahedral holes. The classification of interstitial phases, therefore, is based on radius ratios rather than on the parameters used in the present discussion (Hägg, 1931).

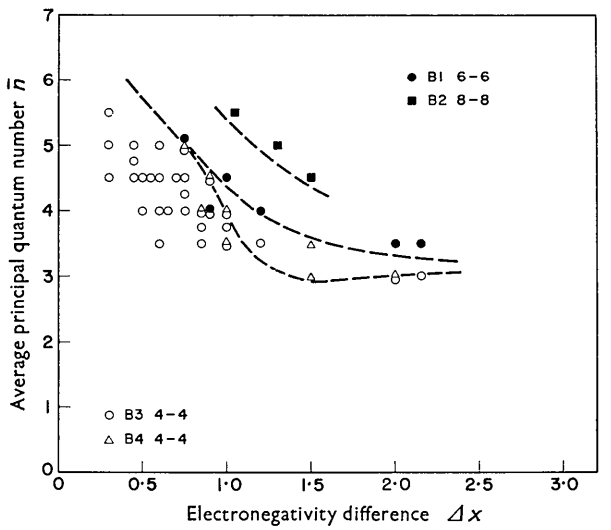

Fig. 4. AX compounds containing B group cations.

The systematic trends found in Fig. 1 are further amplified if the electronic configuration of the component atoms is taken into account. Thus, if in Figs. 3 and 4 we plot the AX compounds containing A group cations (transition elements excluded) and B group cations respectively, we see that the phases with the $B4$ structure now occur in a narrow but well defined region between the $B3$ and $B1$ phases. Moreover, we see that in accordance with their higher coordination and better filling of space, the non-metallic caesium chloride ($B2$) type of phases are located to the right and above the $B1$ phases. In a $\bar{n}$ versus Δx diagram the four structure types ($B1$, $B2$, $B3$, $B4$) therefore are arranged in such a way that along any line of constant $\bar{n}$ the Madelung constants increase with increasing Δx. Many metallic phases also adopt the $B2$ type of structure because of its dense packing. These occur at lower Δx values than the ionic compounds on the $\bar{n}$ versus Δx plot. The filling of space is the same in the $B2$, NaTl ($B32$), Heusler alloy ($L2_1$) and BiF_3 ($D0_3$) structures.

It is worth mentioning here that the alkali halides which adopt the $B1$ rather than the $B2$ structure in spite of the high values of their radius ratios ($r_{cation}/r_{anion} > 0{\cdot}732$) lie well inside the $B1$ region of Fig. 3. It thus seems that the present classification affords an interpretation of the hitherto unexplained structural anomaly found in the alkali halides.

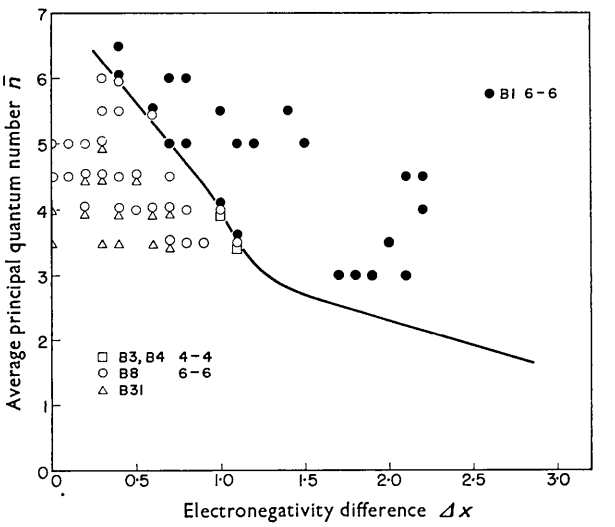

Fig. 5. AX compounds containing transition elements.

Except for bivalent manganese and trivalent iron the transition elements favor an octahedral rather than a tetrahedral coordination. On plotting the AX phases containing transition elements we therefore find, in Fig. 5, that the region formerly occupied by the tetrahedral structures now contains mostly phases crystallizing in the hexagonal nickel–arsenide ($B8$) type of structure or in a distorted form thereof ($B31$ type). In both these structures the cations are octahedrally surrounded by six anions. In the $B8$ structure the cations also have two cation neighbours along the c axis of the crystal and, when the axial ratio is small ($c/a \lesssim 1{\cdot}55$), cation–cation bonds form which further stabilize the $B8$ structure. These cation–cation bonds are responsible for the metallic properties observed in the nickel arsenide phases with small axial ratios (Pearson, 1957).

Some of the nickel arsenide phases are of particular interest. With $\bar{n} = 3{\cdot}5$ and 4 and with $\Delta x = 1{\cdot}1$ and $1{\cdot}0$ respectively, MnS and MnSe lie on the borderlines in Figs. 1 and 5 and accordingly they are polymorphic crystallizing in the $B1$, $B3$ and $B4$ structure types. VS, CrS and VSe, CrSe have the same $\bar{n}$ and Δx values

respectively and thus might be expected to show the same behaviour, whereas they actually adopt a $B8$ structure. The reason for this is that, unlike Mn which may have a tetrahedral coordination when directionally bonded, V and Cr prefer an octahedral coordination and thus do not crystallize in the $B3$ or $B4$ structure. Furthermore, they cannot assume the $B1$ structure which is the stable form of the manganese compounds because the ratios of the cation to anion radii (determining the Me^{2+} radii from the monoxides) lie below the range (0·414–0·732) in which the $B1$ structure is stable. Hence they must adopt the nickel–arsenide type of structure and it is noteworthy that in these compounds the axial ratio c/a is greater than 1·63. As indicated by the relatively large Δx values, the cations carry a considerable charge which leads to a strong cation–cation repulsion and hence to an expansion of the structure along the c axis of the crystal.

The data given in Figs. 1, 2 and 5 show that in a $\bar{n}$ versus Δx diagram there exists a rather sharply defined dividing line between directionally and non-directionally bonded phases of composition AX. Taking into account the remaining valence compounds of this composition—they crystallize in the following rather rare structure types: SiC, HgS, PbO, ZrS, BN, NiS, PtS, CuS, FeSi, TlF, CuO, FeB, TlI, PdS, TlSe, CdSb and MoC–we see (Fig. 6) that the number of different crystal structures to the left of the dividing line greatly exceeds that to the right of it.

The large variety of structure types in the directionally bonded region is a result of the strong dependence of the spatial arrangement of directed bonds on the electronic configuration of the atoms forming the bonds. Once the bonding is essentially nondirectional so that the geometrical factors stipulated by Laves (1956) determine the structure, there is in general no longer any reason for a compound to adopt structures other than the rocksalt or caesium chloride types. Indeed, of the six exceptions in Fig. 6 two (PbO and SnO) crystallize in a distorted caesium chloride structure, while the structures of TlF and TlI are both closely related to the rocksalt structure.

(*b*) *Compounds of composition AX_2, AX_3 and A_2X_3*

The change with increasing values of $\bar{n}$ and/or Δx from more open to more densely packed structures which in the AX phases is apparent in the change from tetrahedral to octahedral structures (Fig. 1) is paralleled in the *anion-rich* AX_2, AX_3 and A_2X_3 phases. This is indicated not only by the higher coordination numbers found on the right-hand side of the solid line in Figs. 7 to 9 but also by the fact that, with the exception of the rather complex $PbCl_2$

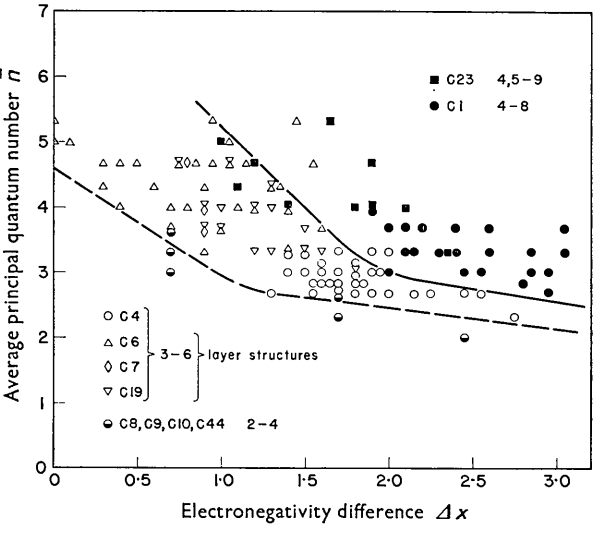

Fig. 7. The structures of AX_2 compounds.

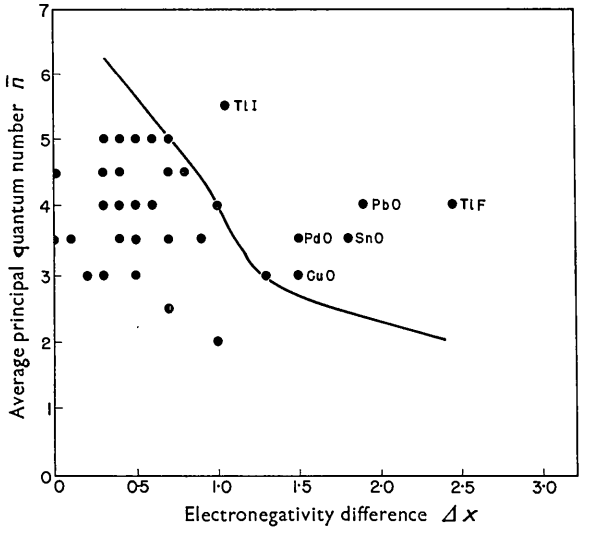

Fig. 6. AX compounds with less common structures.

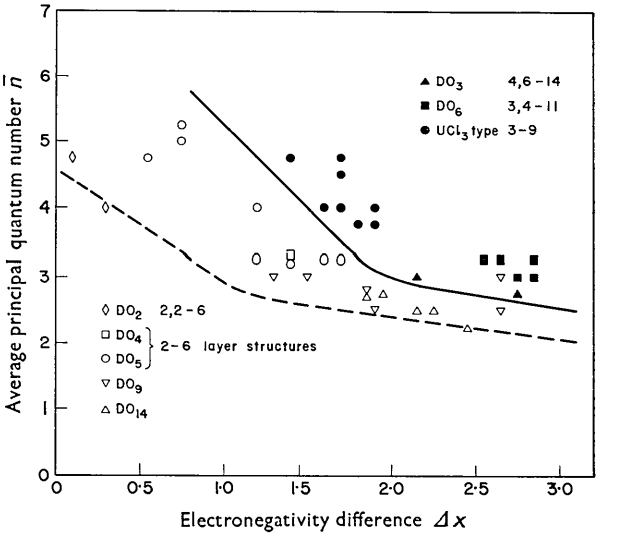

Fig. 8. The structures of AX_3 compounds.

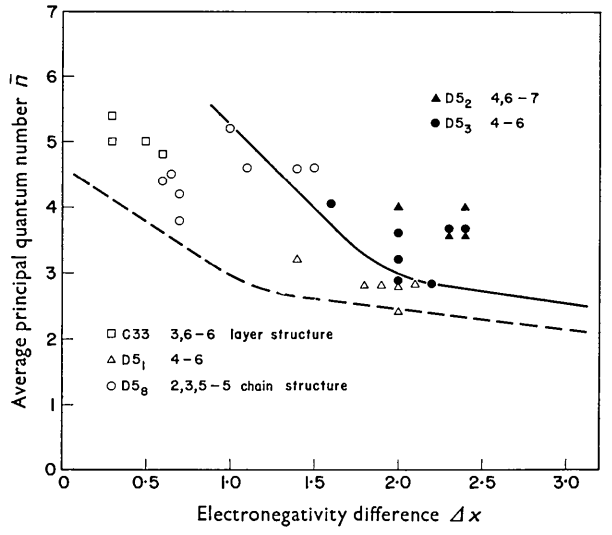

Fig. 9. The structures of A_2X_3 compounds.

($C23$) and UCl_3 structures, the densely packed structures are all based on a *close-packed array of cations*, the holes in which are filled up to various degrees and in different ways by the anions. Obviously, since the number of anions exceeds that of the cations, the degree of filling is rather high, giving rise to densely packed structures. The structure types formed in this manner are listed in Table 1. In contrast to this, most

Table 1. *Structures with close-packed cation arrays*

Phase type	AX_2		AX_3		A_2X_3	
Close-packing of cations	cubic	hex.	cubic	hex.	cubic	hex.
Structure types	$C1$	—	$D0_3$	$D0_6$	$D5_3$	$D5_2$

of the structures lying to the left of the separating line are based on a *close-packed array of anions*. The smaller number of cations leads to a rather low degree of filling of the anion sublattice and hence to the open structures listed in Table 2. It follows from the position

Table 2. *Structures with close-packed anion arrays*

Phase type	AX_2		AX_3		A_2X_3	
Close-packing of anions	cubic	hex.	cubic	hex.	hex.	other
Structure types	$C19$	$C6$	$D0_4$	$D0_5$ $D0_{14}$	$D5_1$	$C33$

of the different anion-rich phases in the $\bar{n}$ versus Δx diagrams that the directional character of the bonds or its absence determines whether the anions or cations lie on a close-packed sublattice: the high filling of space required by nondirectionally bonded phases can be achieved only by placing the cations on the close-packed sites.

We note that in the structures in which the *anions* are closely packed, the cations are usually octahedrally surrounded so that e.g. in the AX_2 compounds a 3–6 coordination results. HgI_2, however, is an exception. In its $C13$ type of structure the anions form a close-packed cubic sublattice in which the cations occupy $\frac{1}{4}$ of the tetrahedral holes. This leads to a 2–4 coordination which normally is met only in the very open framework structures of SiO_2 ($C8$, $C9$, $C10$) and GeS_2 ($C44$) and in the chain structures of SiS_2 ($C42$). In accordance with the general trend these very open structures occur only at the lowest values of $\bar{n}$ and/or Δx and in Fig. 7 they are, therefore, separated from the other AX_2 phases.

In the structures in which the *cations* are closely packed on the other hand, most of the anions sit in the tetrahedral holes. Because the number of anions exceeds that of the cations, the anions are forced into the tetrahedral holes which though somewhat smaller, are twice as numerous as the octahedral holes.

It is very interesting to note that the solid lines separating the densely packed structures from the open structures are the same in each of the diagrams 7 to 9, and we therefore conclude that in the anion-rich compounds with simple atomic ratios, there also exists a strict separation between directionally and nondirectionally bonded phases. This is supported also by the behaviour of the AX_2 phases containing anion pairs. In the pyrite ($C2$) and marcasite ($C18$) structures the anions are tetrahedrally surrounded by one anion and three cations and the cations acquire an octahedral neighbourhood. These coordination configurations clearly indicate the formation of directed bonds and the pyrites and marcasites, therefore, occupy the lower left of the $\bar{n}$ versus Δx diagram (Fig. 10). The calcium carbide ($C11$) structure on the other hand is related to the rocksalt structure, arising from it through the replacement of the anions by anion pairs. It is thus related to the pyrite and marcasite structures in a similar way as the rocksalt structure is related to the zincblende and

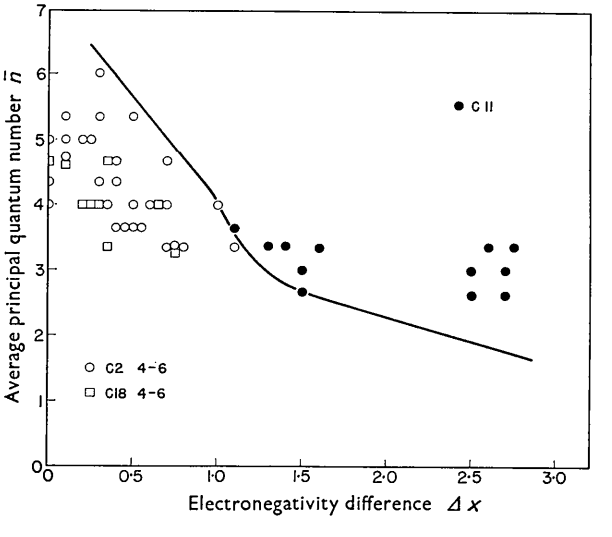

Fig. 10. AX_2 structures containing anion pairs.

Table 3. *Structure types with close-packed anion or cation sublattices*

Type	Representative	Close-packed substructure formed by anions	Close-packed substructure formed by cations	Holes in substructure filled by anions	Holes in substructure filled by cations	Coordination numbers anion	Coordination numbers cation	Remarks
*B*1	NaCl	cubic			all octa.	6	6	Cations also lie on a c.-p. cubic sublattice
*B*3	ZnS	cubic			½ of tetra.	4	4	Cations also lie on a c.-p. cubic sublattice
*B*4	ZnS	hex.			½ of tetra.	4	4	Cations also lie on a c.-p. hex. sublattice
*B*8	NiAs	~hex.			all octa.	6	6	Cations lie on simple hex. sublattice
*C*1	CaF_2		cubic	all tetra.		4	8	Anions lie on simple cubic sublattice
$C1_b$	MgAgAs							Superstructure of *C*1; the components lie on 3 separate interpenetrating c.-p. cubic sublattices
*C*2	FeS_2 Pyrite		cubic	anion pairs located about center of octa.		4	6	Anions tetrahedrally surrounded by 3 cations and 1 anion
*C*6	CdI_2	~hex.			½ of octa.	3	6	3-fold layers $(CdI_2)_n$
*C*11	CaC_2		cubic	tightly bound anion pairs located about center of octa.				Each anion pair has 6 cation neighbours
*C*19	$CdCl_2$	~cubic			½ of octa.	3	6	3-fold layers $(CdCl_2)_n$
$D0_3$	BiF_3		cubic	all tetra. + octa.		4, 6	8+6	
$D0_4$	$CrCl_3$	~cubic			⅓ of octa.	2	6	3-fold layers $(CrCl_3)_n$
$D0_5$	BiI_3	~hex.			⅓ of octa.	2	6	3-fold layers $(BiI_3)_n$
$D0_6$	LaF_3		~hex.	all tetra. + trigonal*		3, 4	11	
$D0_{14}$	AlF_3	~hex.			⅓ of octa.	2	6	Cations lie on a distorted simple cubic sublattice
$D0_{18}$	Na_3As	~hex.			all tetra. + trigonal*	11	3, 4	Essentially anti $D0_6$ structure
$D5_1$	Al_2O_3	~hex.			⅔ of octa.	4	6	
$D5_2$	La_2O_3		~hex.	½ of tetra. + ½ of octa.		4, 6	7	
$D5_3$	Mn_2O_3		~cubic	¾ of tetra.		4	6	Defect Cl structure
$D5_9$	Zn_3P_2	~cubic			¾ tetra.	6	4	Essentially anti $D5_3$ structure

* In the $D0_6$ ($D0_{18}$) structure one third of the anions (cations) are located in the centers of equilateral triangles formed by three cations (anions).

wurtzite structures, being typical of the nondirectionally bonded phases which occur at high $\bar{n}$ and/or Δx values. The line separating the calcium carbide phases from the pyrite and marcasite phases (Fig. 10) coincides with the borderline in Fig. 1.

(c) *Compounds of composition A_2X, A_3X and A_3X_2*

We have seen that in most of the directionally bonded *anion-rich* phases the anions form a close-packed array. This is also true for most of the nonmetallic *cation-rich* phases of composition A_2X, A_3X and A_3X_2 and it might well be taken as an indication of the formation in these phases of directed bonds. However, since here the cations outnumber the anions the degree of filling of holes in the anion sublattice is rather high. In fact a survey of the cation-rich phases shows that the most common structures found among them are the *antitypes* of the densely packed structures listed in Table 1. Thus most of the A_2X compounds adopt the anti-fluorite (*C*1) structure while the A_3X compounds favor either the anti $D0_3$ structure or the $D0_{18}$ structure which is essentially the antitype of the $D0_6$ structure. The A_3X compounds crystallize almost exclusively in the anti $D5_2$, the anti $D5_3$ or the closely related $D5_9$ types. The dense packing in these struc-

Table 4. *Other structure types discussed*

Type	Representative	Coordination numbers anion	cation	Remarks
$B2$	CsCl	8	8	Superlattice of body centered cubic ($A2$) structure
$B16$	GeS	6	6	Distorted rocksalt ($B1$) structures
$B29$	SnS	6	6	
$B31$	MnP			Distorted nickel arsenide ($B8$) structure
$C4$	TiO_2 rutile	3	6	TiO_6 octahedra sharing edges with two neighbouring octahedra form chains. Neighbouring chains touch at the corners of the octahedra
$C7$	MoS_2	3	6	c.-p. planes of anions (A, B) and cations (a, b) are stacked in the sequence $AbABaBAbA\ldots$ i.e. anions and cations together form a distorted c.-p. hexagonal array
$C18$	FeS_2 Marcasite	4	6	Deformed rutile ($C4$). The anions form pairs and the same coordination configurations as in pyrite ($C2$) result
$C23$	$PbCl_2$	4, 5	9	
$C33$	Bi_2Te_2S	3, 6	6	c.-p. planes of anions (A, B, C) and cations (a, b, c) are stacked in the sequence $AbCaBCaBcAbcAbC\ldots$ i.e. anions and cations together form a distorted close-packed cubic lattice
$D0_2$	$CoAs_3$	2, 2	6	Cations lie on a simple cubic sublattice. $\frac{3}{4}$ of cation cubes are filled by square As_4 molecules
$D0_9$	ReO_3	2	6	Cations lie on a simple cubic sublattice. Anions lie on $\frac{3}{4}$ of the sites of a c.-p. cubic lattice
—	UCl_3	3	9	Related to $C23$ in much the same way as $D0_4$ is to $C19$
$D5_8$	Sb_2S_3	2, 3, 5	5	Chains of composition $(Sb_4S_6)_n$ form. The arrangement of the atoms in the chains is reminiscent of the rocksalt ($B1$) structure

tures suggests that they should also be stable when the bonding is nondirectional, and indeed on plotting the anti-$C1$ phases we find them scattered over the whole $\bar{n}$ versus Δx diagram (Fig. 11). Because of the more stringent valence requirements the regions in which the A_3X and A_3X_2 phases occur are somewhat smaller.

We have in Fig. 11 also plotted the ternary phases of composition ABX which crystallize in the $C1$ and $C1_b$ structures. In some of these ternary phases the anions do not sit on the close-packed sites and it has been shown by Junod, Mooser & Schade (1956) that under these circumstances the phases are metallic. In Fig. 10 the metallic phases are clearly separated from the non-metallic phases; they occur only at high $\bar{n}$ and low Δx values i.e. in a region where the bonding is expected to be metallic.

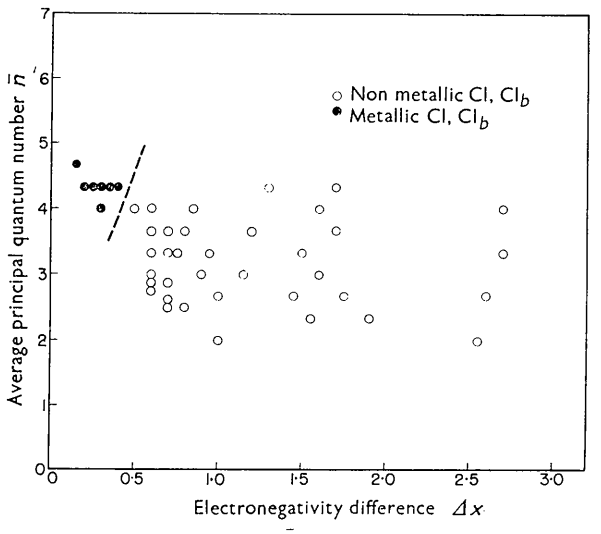

Fig. 11. A_2X phases with the Cl structure.

3. Conclusion

The striking separation in the $\bar{n}$ versus Δx diagram of AX compounds into groups with different crystal structures and the separation of the AX_2, AX_3 and A_2X_3 structures into groups with different packing densities indicates the fundamental importance of a discussion of normal valence compounds in terms of parameters gauging the directional character of the bonds. This is further demonstrated by the relationships found between the structures of anion- and cation-rich phases.

A survey of normal valence compounds of composition AX shows that only a small fraction of them do not crystallize in either the $B1$, $B2$, $B3$, $B4$, $B8$ or $B31$ structures. Diagrams 1 to 5 can therefore be used to predict the structure of a new AX compound with a certainty of about 90%.

APPENDIX

Brief description of the structure types discussed

In many of the structures discussed the anions (cations) lie on close-packed sublattices and the cations (anions)

fill all or part of the tetrahedral and octahedral holes in these sublattices. All these structures are listed in Table 3 which gives the close packing of the sublattices and indicates which holes are filled and to what degree. The remaining structures are listed in Table 4.

References

DEHLINGER, U. (1955). *Theoretische Metallkunde*. Berlin: Springer.

EVANS, R. C. (1939). *An introduction to crystal chemistry*. Cambridge: University Press.

GORDY, W. & THOMAS, W. J. O. (1956). *J. Chem. Phys.* **24**, 439.

HÄGG, G. (1931). *Z. phys. Chem.* B, **12**, 33.

HUME-ROTHERY, W. & RAYNOR, G. V. (1954). *The structures of metals and alloys*. London: Institute of Metals.

JUNOD, P., MOOSER, E. & SCHADE, H. (1956). *Helv. Phys. Acta*, **29**, 193.

KREBS, H. & SCHOTTKY, W. (1954). *Halbleiterprobleme* I, p. 25. Braunschweig: Vieweg.

LAVES, F. (1956). *Theory of alloy phases*, p. 124. The Americ. Soc. for Metals. Cleveland, Ohio.

MOOSER, E. & PEARSON, W. B. (1957). *Helv. Phys. Acta*, **30**, 222.

PEARSON, W. B. (1957). *Canad. J. Phys.* **35**, 886.

PEARSON, W. B. (1959). *Canad. J. Chem.* **37**, 1191.

Acta Cryst. (1959). **12**, 1022

The Crystal Structures of α-V_3S and β-V_3S

BY B. PEDERSEN AND F. GRØNVOLD

Kjemisk Institutt A, Universitetet i Oslo, Blindern, Norway

(*Received* 24 *March* 1959 *and in revised form* 6 *May* 1959)

The structures of a new, dimorphous vanadium sulphide, V_3S, have been determined using single-crystal data.

α-V_3S, which is stable above 950 °C., has a body-centred, tetragonal structure with cell dimensions: $a = 9{\cdot}470$, $c = 4{\cdot}589$ Å. Space group $I\bar{4}2m$ with 8 V in (i) with $x_1 = 0{\cdot}0932$ and $z_1 = \frac{3}{4}$, 8 V in (i) with $x_2 = 0{\cdot}2000$ and $z_2 = \frac{1}{4}$, 8 V in (f) with $x_3 = 0{\cdot}3550$, 8 S in (g) with $x_4 = 0{\cdot}2851$.

β-V_3S, which is stable below 825 °C., has a tetragonal structure with cell dimensions: $a = 9{\cdot}381$, $c = 4{\cdot}663$ Å. Space group $P4_2/nbc$ with 8 V in (j) with $x_1 = 0{\cdot}4080$, 8 V in (j) with $x_2 = 0{\cdot}2028$, 8 V in (i) with $x_3 = 0{\cdot}1486$, 8 S in (h) with $x_4 = 0{\cdot}2171$. (Origin at $\bar{4}$).

Besides being closely related to β-V_3S, the structure of α-V_3S is closely related to that of Ni_3P. The structure of β-V_3S shows relationships to the β-W structure type.

Introduction

In a recent study of the vanadium sulphides (Pedersen, 1958) a subsulphide, V_3S, was identified by means of X-rays. This was unsuspected, as no vanadium sulphide richer in vanadium than VS had been observed by earlier investigators (Vogel & Wüstefeld, 1938; Biltz & Köcher, 1939).

The V_3S samples were made by melting weighed quantities of sulphur and vanadium in stoichiometric proportions at about 1400 °C. in crucibles of pure alumina, placed inside silica tubes which were evacuated and sealed. Depending upon the heat treatment two different forms of V_3S were obtained. Single crystals of the high temperature form (α-V_3S) were found in samples quenched from 1400 °C., and single crystals of the low temperature form (β-V_3S) were found in samples tempered at 825 °C. for about one month. They were probably formed from single crystals of the high temperature form. β-V_3S changed back into α-V_3S after heat treatment at 1150 °C. for six hours. Other experiments showed that α-V_3S was formed at 950 °C. and the transformation is therefore assumed to take place at a temperature between 825 and 950 °C.

Crystal data

The single crystals were needle-shaped with dimensions

$$0{\cdot}04 \times 0{\cdot}04 \times 0{\cdot}4 \text{ mm.}^3 \text{ for } \alpha\text{-}V_3S$$

and

$$0{\cdot}04 \times 0{\cdot}05 \times 0{\cdot}15 \text{ mm.}^3 \text{ for } \beta\text{-}V_3S\,.$$

Oscillation and Weissenberg photographs show that both forms have tetragonal symmetry, Laue symmetry $4/mmm$, with the c-axis along the needle axis. Cell dimensions determined from powder photographs taken with Cu K radiation ($\lambda_{\alpha_1} = 1{\cdot}5405$ Å) and densities, measured pycnometrically at 25·00 °C., are:

α-V_3S	$a = 9{\cdot}470$,	$c = 4{\cdot}589$ Å	$D_o = 5{\cdot}895$ g.cm.$^{-3}$
β-V_3S	$a = 9{\cdot}381$,	$c = 4{\cdot}663$ Å	$D_o = 5{\cdot}939$ g.cm.$^{-3}$.

The observed densities indicate that the unit cell of both forms contain 8 V_3S-groups ($Z_c = 7{\cdot}90$ for α-V_3S and 7·95 for β-V_3S). Missing reflexions are: